



A Journal of the Gesellschaft Deutscher Chemiker

# Angewandte Chemie

GDCh

International Edition

www.angewandte.org

## Accepted Article

**Title:** Reversible Switching of Catalytic Activity by Shuttling an Atom into and out of Au Nanoclusters

**Authors:** Xiao Cai, Govindarajan Saranya, Kangqi Shen, Mingyang Chen, Rui Si, Weiping Ding, and Yan Zhu

This manuscript has been accepted after peer review and appears as an Accepted Article online prior to editing, proofing, and formal publication of the final Version of Record (VoR). This work is currently citable by using the Digital Object Identifier (DOI) given below. The VoR will be published online in Early View as soon as possible and may be different to this Accepted Article as a result of editing. Readers should obtain the VoR from the journal website shown below when it is published to ensure accuracy of information. The authors are responsible for the content of this Accepted Article.

**To be cited as:** *Angew. Chem. Int. Ed.* 10.1002/anie.201903853  
*Angew. Chem.* 10.1002/ange.201903853

**Link to VoR:** <http://dx.doi.org/10.1002/anie.201903853>  
<http://dx.doi.org/10.1002/ange.201903853>

## COMMUNICATION

# Reversible Switching of Catalytic Activity by Shuttling an Atom into and out of Au Nanoclusters

Xiao Cai,<sup>[a]</sup> Govindarajan Saranya,<sup>[b]</sup> Kangqi Shen,<sup>[b]</sup> Mingyang Chen,<sup>\*,[b]</sup> Rui Si,<sup>\*,[c]</sup> Weiping Ding,<sup>[a]</sup> and Yan Zhu<sup>\*,[a]</sup>

**Abstract:** It is a challenge associated with control of catalyst activation and deactivation by only one-central-atom removal and addition, as it is almost impossible to precisely abstract an atom from a conventional catalyst and analyze its catalysis. Here we report that one-central-atom loss in Au<sub>24</sub> enhances catalytic activity in the oxidation of methane compared to Au<sub>25</sub>. More importantly, the activity is readily switchable through shuttling the central atom into Au<sub>24</sub> and out of Au<sub>25</sub>. This work will serve as a starting point for design rules on how to control catalytic performance of a catalyst by an atom alteration.

Every atom of a catalyst can be directly or indirectly involved in a reaction process. However, it is difficult to distinguish the contribution of individual atom on different sites in a catalyst to the catalytic performance, as it is challenging to control the catalyst activation and deactivation by addition or removal of an atom. In the subnanometre size regime, every atom of a catalyst can have a potential influence on the overall performance,<sup>[1]</sup> and hence it is necessary to gain fundamental insights into catalysis of one atom on a special site. With the successful attainment of atomically precise metal nanoclusters capped by ligands,<sup>[2]</sup> where an atom of a nanocluster can be replaced by a foreign atom without altering the atomic structure of the nanocluster,<sup>[3]</sup> an opportunity for unravelling catalysis of one doping atom has been provided. For example, it has been reported that replacing the central atom of Au nanoclusters with a platinum atom caused a drastic increase in the catalytic activity for selective oxidation of styrene or the hydrogenation production.<sup>[4]</sup> The Au<sub>25</sub> nanocluster doped by a Pd atom showed an enhancement in aerobic alcohol oxidation.<sup>[5]</sup> Our group found that the central doping of a foreign atom (Au, Pd or Pt) into the Ag<sub>25</sub> nanocluster can have a substantial influence on the catalytic reactivity in the carboxylation reaction of CO<sub>2</sub> with terminal alkyne.<sup>[6]</sup> These studies indicate that the alteration of a catalyst by a foreign dopant that leads to a heterometal catalyst can drastically change the catalytic properties of the original catalyst. In particular, recent success in shuttling single gold atom into [Au<sub>24</sub>(PPh<sub>3</sub>)<sub>10</sub>(SC<sub>2</sub>H<sub>4</sub>Ph)<sub>5</sub>Cl<sub>2</sub>]<sup>+</sup> (abbreviated as Au<sub>24</sub>,

hereafter) and out of [Au<sub>25</sub>(PPh<sub>3</sub>)<sub>10</sub>(SC<sub>2</sub>H<sub>4</sub>Ph)<sub>5</sub>Cl<sub>2</sub>]<sup>2+</sup> (abbreviated as Au<sub>25</sub>, hereafter)<sup>[7]</sup> allows us to explore how the catalytic properties of a homometal catalyst are dominated by addition or removal of a single metal atom.

Au<sub>24</sub> and Au<sub>25</sub> nanoclusters have identical surface atomic organization, as shown in Figure 1a, which can be viewed as two vertex-sharing Au<sub>13</sub> icosahedrons coordinated to five thiolate linkages; the top and bottom Au<sub>5</sub> pentagons are linked by ten triphenylphosphine; the two apex gold atoms are bound to two Cl atoms. It is noted that the only difference of Au<sub>24</sub> and Au<sub>25</sub> is that Au<sub>24</sub> misses the central atom. Here we demonstrate that one-central-atom loss in the Au<sub>24</sub> nanocluster enables better catalytic activity in the methane oxidation toward methanol compared to the Au<sub>25</sub> nanocluster. More importantly, the activation and deactivation can be reversibly switched by losing the central atom and filling the central vacancy, which effectively avoids the irreversibility of catalytic capability and improves the durability.

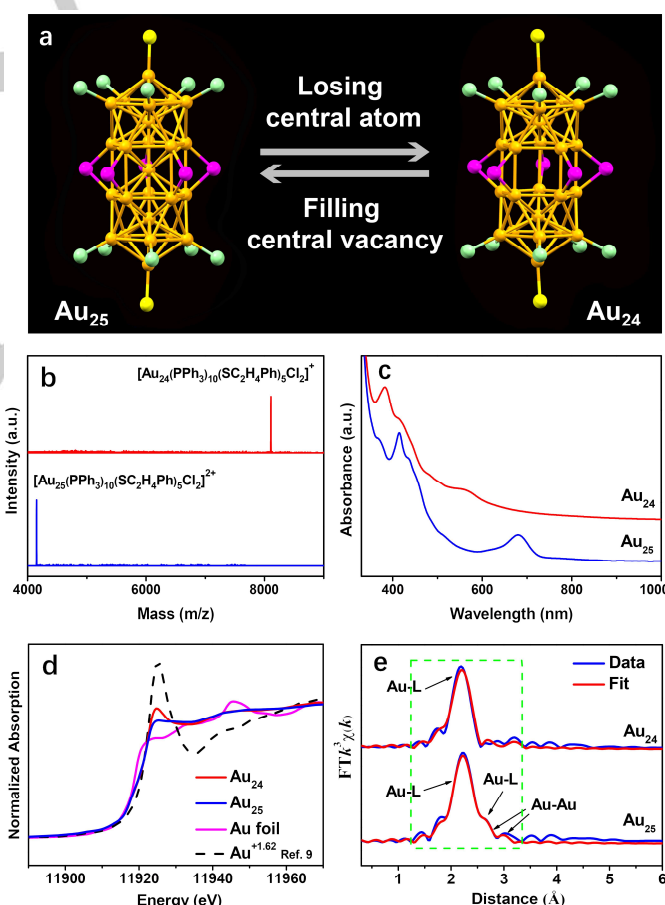


**Figure 1.** (a) Atomic structures of Au<sub>24</sub> with the central vacancy and Au<sub>25</sub> with the central atom (Color label: Au, orange; S, pink; Cl, yellow; P, green. C and H atoms are omitted for clarity). (b) ESI-MS spectra of Au<sub>24</sub> and Au<sub>25</sub>. (c) UV-vis spectra of Au<sub>24</sub> and Au<sub>25</sub>. (d) XANES and (e) EXAFS profiles of Au<sub>24</sub> and Au<sub>25</sub>. (L = P/S; Green dash rectangle frame indicates the fitted R range.)

- [a] X. Cai, Prof. W. Ding, Prof. Y. Zhu  
Key Lab of Mesoscopic Chemistry, School of Chemistry and Chemical Engineering, Nanjing University, Nanjing 210093, China  
E-mail: zhuyan@nju.edu.cn
- [b] G. Saranya, K. Shen, Prof. M. Chen  
Beijing Computational Science Research Center, Beijing 100193, China  
E-mail: mychen@csrc.ac.cn
- [c] Prof. R. Si  
Shanghai Radiation Facility, Shanghai Institute of Applied Physics, Chinese Academy of Sciences, Shanghai 201204, China  
E-mail: sirui@sinap.ac.cn

Supporting information for this article is given via a link at the end of the document.

## COMMUNICATION

The two gold nanoclusters were analyzed by electrospray ionization mass spectrometry (ESI-MS) and determined to be  $\text{Au}_{24}(\text{PPh}_3)_{10}(\text{SC}_2\text{H}_4\text{Ph})_5\text{Cl}_2$  and  $\text{Au}_{25}(\text{PPh}_3)_{10}(\text{SC}_2\text{H}_4\text{Ph})_5\text{Cl}_2$  (Figure 1b). The UV-vis absorption spectrum of  $\text{Au}_{24}$  showed prominent peaks at 382 and 560 nm, while the absorption peaks in  $\text{Au}_{25}$  were located at 415 and 670 nm (Figure 1c). X-ray photoelectron spectroscopy (XPS) studies showed that the Au 4f binding energies of  $\text{Au}_{24}$  were positively shifted, compared to  $\text{Au}_{25}$  (Figure S1 shown in Supporting Information). The presence of  $\text{Au}^0$  and  $\text{Au}^+$  was in the Au 4f spectra of the two nanoclusters, in which the  $\text{Au}^+$  species appeared on the surface of nanoclusters, mainly owing to the electron donation occurring from the surface Au atoms to the ligands.<sup>[8]</sup> The mole ratio of  $\text{Au}^+$  to  $\text{Au}^0$  was 0.68 for  $\text{Au}_{24}$  and 0.52 for  $\text{Au}_{25}$ , respectively. The data suggest that  $\text{Au}_{24}$  carried more positive charge in comparison with  $\text{Au}_{25}$ .

The changes in the gold charge state were also monitored by X-ray absorption near edges structure (XANES) studies (Figure 1d), which indicated that the average charge state of  $\text{Au}_{24}$  (+0.53) was more positive than that of  $\text{Au}_{25}$  (+0.35) by the aids of linear combination fits (Figure S2).<sup>[9]</sup> Furthermore, local coordination environments in  $\text{Au}_{24}$  and  $\text{Au}_{25}$  were probed by extended X-ray absorption fine structure (EXAFS) experiments. Besides the capped ligands, as shown in Figure 1e,  $\text{Au}_{25}$  showed an extra Au-Au contribution (split peaks at ca. 2.75 Å, more details in Figure S2 and Table S1), uniquely originated from the center gold atom. Other gold-gold bonds in either  $\text{Au}_{24}$  or  $\text{Au}_{25}$  disappeared in EXAFS spectra, probably due to the thermal fluctuation of Au-Au bonds at room temperature.<sup>[10]</sup> Note that the Au-Au bonds in small Au clusters were visible only when the EXAFS data were collected at low temperature (8 K).<sup>[11]</sup>

One-central-atom loss in the  $\text{Au}_{24}$  nanocluster induced a significant perturbation to the electronic structure, which may render different catalytic properties. Therefore, catalysis of the  $\text{Au}_{24}$  and  $\text{Au}_{25}$  nanoclusters was explored, in which catalytic conversion of methane was used as a model reaction. As shown in Figure 2a, the  $\text{Au}_{24}$  catalyst was more effective than the  $\text{Au}_{25}$  catalyst for catalytic oxidation of methane with  $\text{H}_2\text{O}_2$ . Notably, both  $\text{Au}_{24}$  and  $\text{Au}_{25}$  nanoclusters efficiently converted methane to methanol. As presented in Figure 2b, typical Au nanoparticles manifested in Figure S3-4 had no catalytic activity under identical experimental conditions.

Considering that the ligand-capped  $\text{Au}_{24}$  and  $\text{Au}_{25}$  contained carbon sources, the comparison experiments were done. Either  $\text{CH}_4$  or  $\text{H}_2\text{O}_2$  was introduced and no product was detected (Figure 2b).  $^{13}\text{C}$  nuclear magnetic resonance (NMR) studies further supported the product derived from methane and meanwhile confirmed the liquid product assigned to methanol (Figure S5). The results not only rule out methanol evolution from the Au's organic ligands, but also verify that the  $\text{Au}_{24}$  and  $\text{Au}_{25}$  catalysts can convert methane to methanol.

More interestingly, the performances of recycled catalysts gave us the new aspects about the reversible activity of the two nanoclusters in the reaction.  $\text{Au}_{24}$  was more active but less stable than  $\text{Au}_{25}$  and with cycles  $\text{Au}_{24}$  went through a continued slowdown in activity close to  $\text{Au}_{25}$  (Figure 2c). Our studies showed that the structure of  $\text{Au}_{24}$  appeared to be rearranged under the existence of  $\text{H}_2\text{O}_2$ . The evolution of the UV-vis spectra of the  $\text{Au}_{24}$  and  $\text{Au}_{25}$  in  $\text{H}_2\text{O}_2$  not only showed that the atomicity of  $\text{Au}_{25}$  was rather preserved, but also revealed that  $\text{Au}_{24}$  underwent a structure transformation into  $\text{Au}_{25}$  (Figure S6), which was also supported by ESI-MS spectra (Figure S7). Notably, inspired by

the last stage of  $\text{Au}_{24}$  synthesis, we envisioned a structure regeneration of  $\text{Au}_{24}$  by the destroyed  $\text{Au}_{24}$  (in fact it had been  $\text{Au}_{25}$ ) reacting with the excess  $\text{PPh}_3$ . As expected, the conversion between  $\text{Au}_{24}$  and  $\text{Au}_{25}$  was completely reversible:  $\text{Au}_{25}$  was converted back to  $\text{Au}_{24}$  (Figure S8) and the activity was recovered (Figure 2d). The phenomena clearly indicate that the activity is readily switchable through shuttling the central atom into  $\text{Au}_{24}$  and out of  $\text{Au}_{25}$ . The reversible activity is of particular importance to avoid the irreversible inactivation and the fading of cycle life.

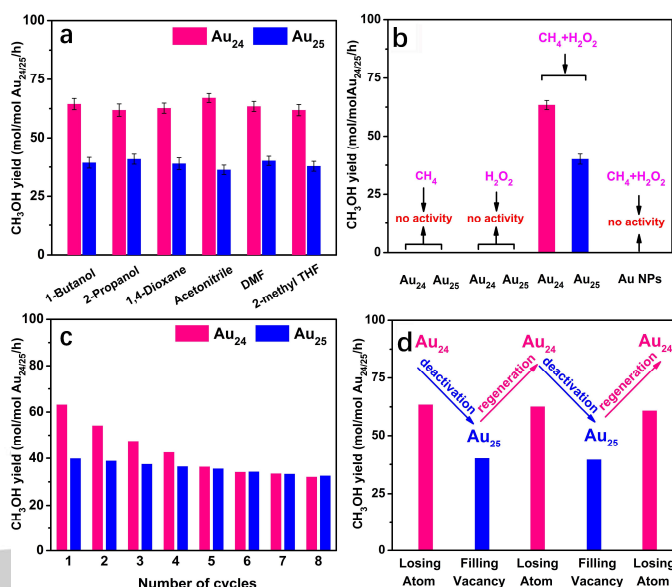


**Figure 2.** (a) Catalytic performance of methane oxidation over the  $\text{Au}_{24}$  and  $\text{Au}_{25}$  catalysts in the different solvents. (b) Comparison of catalytic properties of the gold catalysts under different reaction conditions. (c) Recyclability of  $\text{Au}_{24}$  and  $\text{Au}_{25}$ . (d) Activity reversible behavior of  $\text{Au}_{24}$  and  $\text{Au}_{25}$ . Reaction conditions: 1 mg gold, 0.3 M  $\text{H}_2\text{O}_2$ , 15 ml DMF, 2 MPa  $\text{CH}_4$ , 50 °C.

To understand catalysis of one-central-atom removal and addition, the reaction mechanism of methane oxidation catalyzed by the  $\text{Au}_{24}$  and  $\text{Au}_{25}$  catalysts was investigated in detail. Firstly the potential radical species were detected by electron paramagnetic resonance spectroscopy (EPR) with 5,5-dimethylpyrroline-N-oxide (DMPO) as a radical trapping agent. As shown in Figure 3a, before the introduction of methane, a characteristic signal (1:2:2:1) corresponding to DMPO-OH adduct was found, revealing the presence of hydroxyl radicals. After the introduction of methane and  $\text{H}_2\text{O}_2$  in the system for 10 min, only •OH adduct with DMPO was observed. When the gold clusters were added to the system containing methane and  $\text{H}_2\text{O}_2$ , besides •OH adduct (asterisk symbol), • $\text{CH}_3$  adduct (well symbol) with DMPO was also detected (Figure 3a). Further, the addition of the hydroxyl radical scavenger ( $\text{Na}_2\text{SO}_3$ ) into the reactions led to the decrease of methane conversion (Figure S9). It indicates that hydroxyl radicals are the major active oxygen species.

To determine the potential intermediate species adsorbed over the  $\text{Au}_{24}$  and  $\text{Au}_{25}$  catalysts in the oxidation of methane, attenuated total reflection infrared (ATR-IR) spectra were performed by exposure of the two nanoclusters to methane and  $\text{H}_2\text{O}_2$ . From Figure 3b, the two bands were visible at 2966 and 2921  $\text{cm}^{-1}$ , which are assigned to the asymmetric C-H stretching vibrations of methoxy groups.<sup>[12]</sup> The band at 2940  $\text{cm}^{-1}$  is assigned to an overtone deformation vibration of methoxy groups and the band at 2824  $\text{cm}^{-1}$  is associated with a symmetric C-H

## COMMUNICATION

stretching vibration of methoxy groups.<sup>[13]</sup> The bands at 2980 and 2866  $\text{cm}^{-1}$  can be assigned to asymmetric and symmetric C-H stretches of methoxy groups produced by the reaction of methanol with hydroxyl groups, respectively.<sup>[14]</sup> The  $\nu_s(\text{C-H})$  mode of  $\text{OCH}_3$  groups appearing at 2844  $\text{cm}^{-1}$  was also detected.<sup>[15]</sup> The results imply that the reactions of methane with  $\text{H}_2\text{O}_2$  over the two nanoclusters are accompanied with the formation of methoxy species.

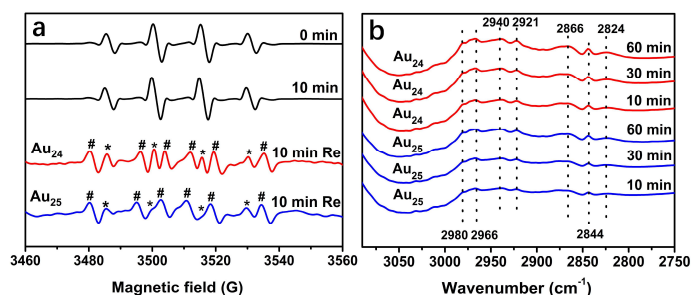


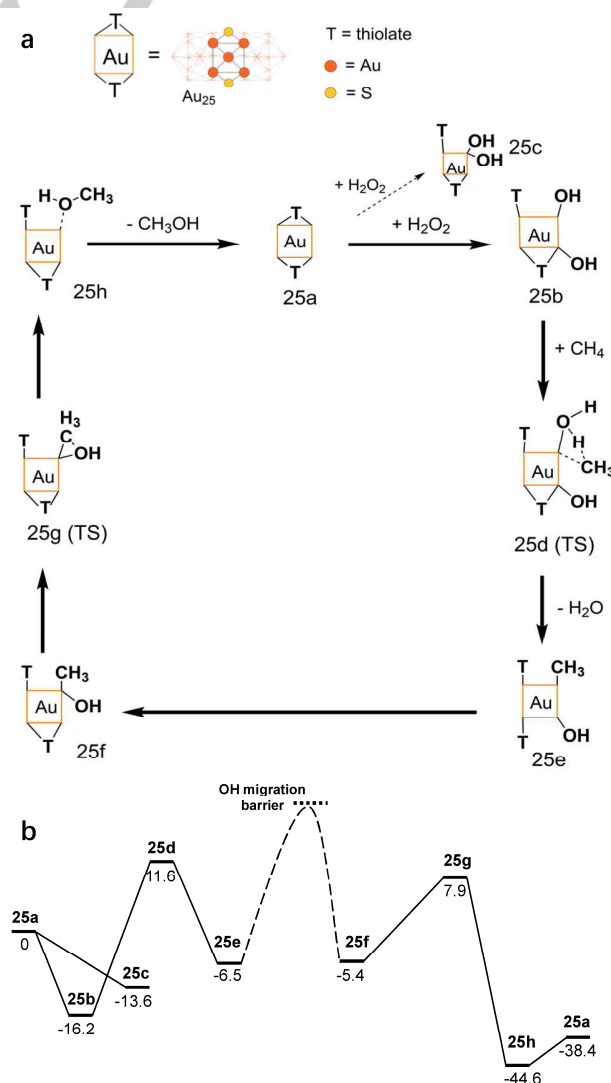
**Figure 3.** (a) EPR spectra of  $\text{CH}_4$  reaction with  $\text{H}_2\text{O}_2$ : spectra obtained from  $\text{H}_2\text{O}_2$  solution before the introduction of  $\text{CH}_4$  (0 min); after 10 min reaction of  $\text{CH}_4$  and  $\text{H}_2\text{O}_2$  without the catalyst; after 10 min reactions of  $\text{CH}_4$  and  $\text{H}_2\text{O}_2$  catalyzed by  $\text{Au}_{24}$  and  $\text{Au}_{25}$ . (b) ATR-IR spectra of  $\text{CH}_4$  reaction with  $\text{H}_2\text{O}_2$  catalyzed by  $\text{Au}_{24}$  and  $\text{Au}_{25}$ .

Furthermore, the reaction pathways and energy profiles for the methane oxidation over  $\text{Au}_{24}$  and  $\text{Au}_{25}$  were explored by Density functional theory (DFT) calculations. Initially, a  $\text{H}_2\text{O}_2$  dissociatively adsorbs as two  $\cdot\text{OH}$  at two surface Au sites. All the surface Au atoms except the two apex Au atoms bonded to Cl can adsorb OH exothermically ( $E_{\text{ads}} \approx -30$  kcal/mol). The adsorbed OH on the intact catalyst cannot initiate  $\text{CH}_4$  activation. Instead, OH at open Au of the partial cleavage of the Au-thiol-Au bridge can react with  $\text{CH}_4$  (**25b** and **24b** in Figure 4a and 4c; the optimized geometries in Figure S10), with  $E_{\text{ads}}(\text{OH}) = \sim 20$  kcal/mol. The reaction pathway for the less reactive  $\text{Au}_{25}$  was first considered (Figure 4a and 4b).  $\text{CH}_4$  is activated via a triangular transition state (TS) **25d**, with the barrier height  $\Delta H^\ddagger = \sim 30$  kcal/mol, leading to **25e**. The partial cleavage exposes a low-coordination surface Au and provides enough reaction space around the singly adsorbed Au-OH to activate  $\text{CH}_4$  and accept  $\cdot\text{CH}_3$  from  $\text{CH}_4$  activation. Alternatively, if two OH are adsorbed at the partial cleavage (**25c**), the  $\text{CH}_4$  activation is suppressed. For  $\text{CH}_3$  and OH to recombine in **25e**, OH must migrate to adjacent Au that adsorbs  $\text{CH}_3$ , as the orientation of  $\text{HO-Au1-Au2-CH}_3$  forbids the two-site recombination ( $\angle\text{Au1-Au2-C} = 125^\circ$ ). The OH migration can be done via bending  $\angle\text{Au2-Au1-O}$ , leading to **25f**. A rigid scan of  $\angle\text{Au2-Au1-O}$  shows the migration requires  $>40$  kcal/mol to overcome the barrier (Figure S11a). The successive one-site recombination of  $\text{CH}_3$  and OH (**25f**  $\rightarrow$  **25h** via TS **25g**) has a low barrier of  $\sim 15$  kcal/mol. The so-formed  $\text{CH}_3\text{OH}$  in **25h** is weakly adsorbed ( $E_{\text{ads}} = \sim 5$  kcal/mol).

The reaction with  $\text{Au}_{24}$  could take a pathway similar to the  $\text{Au}_{25}$  pathway, with exactly alike energetics (black paths in Figure 4c and 4d). If so,  $\text{Au}_{24}$  and  $\text{Au}_{25}$  would exhibit similar catalytic behaviors, which contradicts the experimental results. DFT reveals that the central vacancy enables two additional shortcut pathways (red and blue paths in Figure 4c and 4d) that can enhance catalysis of  $\text{Au}_{24}$ . A surface Au can facilitate migrate to fill the vacancy at the rod center (Figure S12) with  $\Delta H^\ddagger = 9$  kcal/mol. The resulting  $\text{Au}_{24}$  complexes are denoted as M- $\text{Au}_{24}$  complexes

and are indicated by \* in their labels. Both shortcut pathways avoid the rate-limiting OH migration barrier along **24e**  $\rightarrow$  **24f**. The first shortcut connects **24a** and **24f**, along which the one-site  $\text{CH}_4$  activation (**24b**  $\rightarrow$  **24e**) and succeeding OH migration are replaced by a two-site reaction (**24b\***  $\rightarrow$  **24f** via TS **24d\*** with  $\Delta H^\ddagger = 30$  kcal/mol). The second shortcut deviates from **24e** and terminates at **24h**, where the one-site  $\text{CH}_3\text{-OH}$  recombination (**24f**  $\rightarrow$  **24h**) and preceding OH migration are replaced by a two-site  $\text{CH}_3\text{-OH}$  recombination (**24e\***  $\rightarrow$  **24h** via TS **24g\*** with  $\Delta H^\ddagger = 27$  kcal/mol) that directly leads to the  $\text{CH}_3\text{OH}$  product (**24h**). The two-site reactions are enabled by suitable Au-adsorbate orientations at the central site of M- $\text{Au}_{24}$ . For example, in **24e\***,  $\angle\text{Au1-Au2-C}$  of the  $\text{HO-Au1-Au2-CH}_3$  site is  $86^\circ$ , so bending  $\angle\text{Au2-Au1-O}$  directly leads to TS of two-site recombination reaction (Figure S11b). Conversely, bending  $\angle\text{Au2-Au1-O}$  in **24e** and **25e** only leads to a pre-recombination intermediates.

In addition, the isomerization from  $\text{Au}_{24}$  to M- $\text{Au}_{24}$  also increases the mobility of OH adsorbate, and enhances  $\text{CH}_3\text{-OH}$  recombination. For  $\text{Au}_{25}$ , the trajectory of OH connects two surface Au atoms on the  $\text{Au}_5$  pentagon ring of the icosahedral  $\text{Au}_{12}$  sphere and is always under substantial steric effect of Au-PPh<sub>3</sub>, indicated by the barrier at  $\angle\text{Au-Au-OH} = \sim 90^\circ$  during the **25e**  $\rightarrow$  **25f** rigid scan (Figure S11a). For M- $\text{Au}_{24}$  **24e\***  $\rightarrow$  **24g\***





## COMMUNICATION

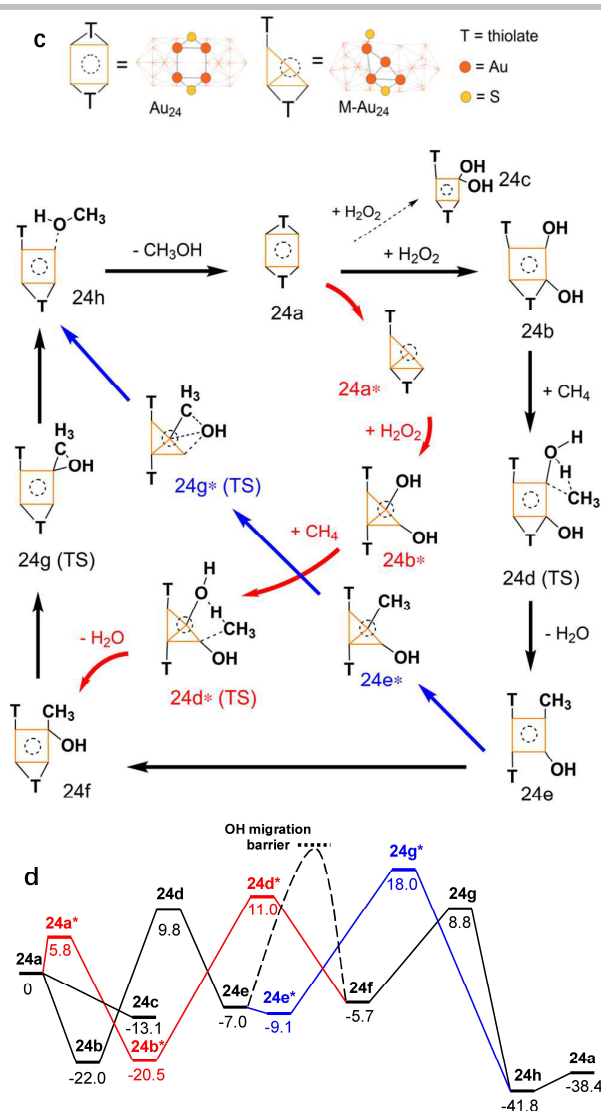


**Figure 4.** Proposed catalytic mechanism and predicted reaction enthalpy profiles for the methane oxidation on (a, b)  $\text{Au}_{25}$  and (c, d)  $\text{Au}_{24}$  at the DFT PBE/LANL2DZ level with  $[\text{Au}_{24/25}(\text{PPh}_3)_2(\text{SCH}_3)_2(\text{SC}_2\text{H}_4\text{Ph})_3\text{Cl}_2]^{+2+}$  models using GAUSSIAN09 program. Reaction enthalpies are at 0 K in kcal/mol.  $\text{Au}_{24}$  and  $\text{Au}_{25}$  complexes are labeled as  $24\text{N}$  and  $25\text{N}$ ,  $\text{N} = \text{a, b, c, etc.}$ , and  $\text{M-Au}_{24}$  complexes are denoted as  $24\text{N}^*$ . All of the corresponding optimized geometries can be found in Figure S10. Black paths indicate the reaction pathways for  $\text{Au}_{25}$  and  $\text{Au}_{24}$  without involving the central vacancy, whereas the red and blue paths indicate the shortcut-pathways that involve  $\text{M-Au}_{24}$ .

transition, the trajectory of OH connects a surface Au and the central Au, and the steric effect on OH decreases as OH moves towards the central Au.

In brief, DFT calculations show that the methane to methanol conversion on the  $\text{Au}_{24}$  and  $\text{Au}_{25}$  catalysts are facilitated by the heterogeneous active sites on the surface of the nanoclusters. The  $\text{PPh}_3$  and  $\text{SC}_2\text{H}_4\text{Ph}$  protected Au sites can adsorb free  $\bullet\text{OH}$  in the reaction. The partial cleaved bridge Au sites induced by OH insertion can promote  $\text{CH}_4$  activation, and adsorb the resulting  $\text{CH}_3$ . The  $\text{M-Au}_{24}$  isomer of  $\text{Au}_{24}$ , resulting from the migration of the central vacancy in  $\text{Au}_{24}$ , enables the two-site reaction steps that enhance catalysis of  $\text{Au}_{24}$ , which can be insightful in designing catalytic reactions that involve two small fragments. More supplemental discussion about the structural and electronic properties of  $\text{Au}_{24}$  and  $\text{Au}_{25}$  at DFT level, geometry optimizations

for intermediates, and transition states can be found in Supporting Information.

In summary, our studies show that the alteration of a gold nanocluster by one central atom can significantly change the catalytic properties. The catalytic activity can be switched by one-central-atom removal and addition. The work apparently impacts one's understanding of the contributions of individual atoms on different sites in a catalyst to the catalytic performance and provides design rules on how to control the catalytic properties of a catalyst by one-atom removal and addition.

## Acknowledgements

We acknowledge financial support from National Natural Science Foundation of China (21773109, 91845104, and U1530401) and Fundamental Research Funds for the Central Universities. We thank Prof. Rongchao Jin from Carnegie Mellon University for helpful discussion.

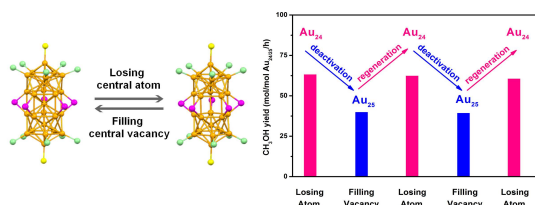
**Keywords:** atom • vacancy •  $\text{Au}_{25}$  •  $\text{Au}_{24}$  • catalysis

- [1] M. M. Shoshani, S. A. Johnson, *Nat. Chem.* **2017**, 9, 1282-1285.
- [2] a) P. D. Jadzinsky, G. Calero, C. J. Ackerson, D. A. Bushnell, R. D. Kornberg, *Science* **2007**, 318, 430-433; b) A. Desireddy, B. E. Conn, J. Guo, B. Yoon, R. N. Barnett, B. M. Monahan, K. Kirschbaum, W. P. Griffith, R. L. Whetten, U. Landman, T. P. Bigioni, *Nature* **2013**, 501, 399-402; c) M. Azubel, J. Koivisto, S. Malola, D. Bushnell, G. L. Hura, A. L. Koh, H. Tsunoyama, T. Tsukuda, M. Pettersson, H. Häkkinen, R. D. Kornberg, *Science* **2014**, 345, 909-912; d) C. Zeng, Y. Chen, K. Kirschbaum, K. J. Lambright, R. Jin, *Science* **2016**, 354, 1580-1584; e) Q. Yao, V. Fung, C. Sun, S. Huang, T. Chen, D. Jiang, J. Y. Lee, J. Xie, *Nat. Commun.* **2018**, 9, 1979; g) X. Wan, Z. Guan, Q. Wang, *Angew. Chem. Int. Ed.* **2017**, 56, 11494-11497.
- [3] a) M. S. Bootharaju, C. P. Joshi, M. R. Parida, O. F. Mohammed, O. M. Bakr, *Angew. Chem. Int. Ed.* **2016**, 55, 922-926; b) C. Yao, Y. Lin, J. Yuan, L. Liao, M. Zhu, L. Weng, J. Yang, Z. Wu, *J. Am. Chem. Soc.* **2015**, 137, 15350-15353; c) Y. Negishi, W. Kurashige, Y. Kobayashi, S. Yamazoe, N. Kojima, M. Seto, T. Tsukuda, *J. Phys. Chem. Lett.* **2013**, 4, 3579-3583; d) J. Yan, H. Su, H. Yang, S. Malola, S. Lin, H. Häkkinen, N. Zheng, *J. Am. Chem. Soc.* **2015**, 137, 11880-11883.
- [4] a) H. Qian, D. Jiang, G. Li, C. Gayathri, A. Das, R. R. Gil, R. Jin, *J. Am. Chem. Soc.* **2012**, 134, 16159-16162; b) K. Kwak, W. Choi, Q. Tang, M. Kim, Y. Lee, D. Jiang, D. Lee, *Nat. Commun.* **2017**, 8, 14723.
- [5] S. Xie, H. Tsunoyama, W. Kurashige, Y. Negishi, T. Tsukuda, *ACS Catal.* **2012**, 2, 1519-1523.
- [6] Y. Liu, X. Chai, X. Cai, M. Chen, R. Jin, W. Ding, Y. Zhu, *Angew. Chem. Int. Ed.* **2018**, 57, 9775-9779.
- [7] S. Wang, H. Abroshan, C. Liu, T. Luo, M. Zhu, H. J. Kim, N. L. Rosi, R. Jin, *Nat. Commun.* **2017**, 8, 848.
- [8] Y. Negishi, K. Nobusada, T. Tsukuda, *J. Am. Chem. Soc.* **2005**, 127, 5261-5270.
- [9] L. Guo, P. Du, X. Fu, C. Ma, J. Zeng, R. Si, Y. Huang, C. Jia, Y. Zhang, C. Yan, *Nat. Commun.* **2016**, 7, 13481.
- [10] P. Zhang, *J. Phys. Chem. C* **2014**, 118, 25291-25299.
- [11] S. Yamazoe, S. Takano, W. Kurashige, T. Yokoyama, K. Nitta, Y. Negishi, T. Tsukuda, *Nat. Commun.* **2016**, 7, 10414.
- [12] B. R. Wood, J. A. Reimer, A. T. Bell, M. T. Janicke, K. C. Ott, *J. Catal.* **2004**, 225, 300-306.
- [13] S. Kameoka, T. Nobukawa, S. I. Tanaka, S. I. Ito, K. Tomishige, K. Kunimori, *Phys. Chem. Chem. Phys.* **2003**, 5, 3328-3333.
- [14] S. M. Campbell, X. Jiang, R. F. Howe, *Micropor. Mater.* **1999**, 29, 91-108.
- [15] R. Tumma, S. Siliveri, H. B. Vamaraju, M. R. Bommineni, *J. Pharm. Res.* **2017**, 11, 895-902.

## COMMUNICATION

Entry for the Table of Contents (Please choose one layout)

## COMMUNICATION



Our work shows that the catalytic performance of a catalyst can be significantly altered by one-central-atom removal and addition. Shuttling one-central-atom into the Au<sub>24</sub> and out of the Au<sub>25</sub> is indeed accompanied by an enhancement and detriment in catalytic capability.

Xiao Cai,<sup>[a]</sup> Govindarajan Saranya,<sup>[b]</sup>  
Kangqi Shen,<sup>[b]</sup> Mingyang Chen,<sup>\*,[b]</sup> Rui  
Si,<sup>\*,[c]</sup> Weiping Ding,<sup>[a]</sup> and Yan Zhu<sup>\*,[a]</sup>

Page No. 1 – Page No. 4

**Reversible Switching of Catalytic  
Activity by Shuttling an Atom into  
and out of Au Nanoclusters**